Quantum Yield Measurements of Short-Lived Photoactivation Intermediates in DNA Photolyase: Toward a Detailed Understanding of the Triple Tryptophan Electron Transfer Chain

ARTICLE *in* THE JOURNAL OF PHYSICAL CHEMISTRY A · DECEMBER 2009

Impact Factor: 2.69 · DOI: 10.1021/jp9093589 · Source: PubMed

Polarized Transient Absorption To Resolve Electron Transfer between Tryptophans in DNA Photolyase

Martin Byrdin,*,†,‡ Sandrine Villette,†,‡,§ Agathe Espagne,†,‡,∥ Andre P. M. Eker,⊥ and Klaus Brettel†,‡

Laboratoire de Photocatalyse et Biohydrogène, iBiTecS, CEA, 91191 Gif sur Yvette, France, URA 2096, CNRS, 91191 Gif sur Yvette, France, and Department of Cell Biology and Genetics, MGC, Erasmus University Medical Centre, PO Box 2040, Rotterdam, 3000 CA, The Netherlands

Received: December 4, 2007; Revised Manuscript Received: March 11, 2008

Transient absorption spectroscopy is a powerful tool for studying biological electron-transfer chains, provided that their members give rise to distinct changes of their absorption spectra. There are, however, chains that contain identical molecules, so that electron transfer between them does not change net absorption. An example is the chain flavin adenine dinucleotide (FAD)−W382−W359−W306 in DNA photolyase from *E. coli*. Upon absorption of a photon, the excited state of $FADH^{\bullet}$ (neutral FAD radical) abstracts an electron from the tryptophan residue W382 in ∼30 ps (monitored by transient absorption). The cation radical $W382^{\bullet+}$ is presumably reduced by W359 and $W359^{\bullet+}$ by W306. The latter two reactions could not be monitored directly so far because the absorption changes of the partners compensate in each step. To overcome this difficulty, we used linearly polarized flashes for excitation of $FADH^{\bullet}$, thus inducing a preferential axis in the a priori unoriented sample (photoselection). Because W359 and W306 are very differently oriented within the protein, detection with polarized light should allow us to distinguish them. To demonstrate this, W306 was mutated to redox-inert phenylalanine. We show that the resulting anisotropy spectrum of the initial absorption changes (measured at 10 ns time resolution) is in line with W359 being oxidized. The corresponding spectrum in wildtype photolyase is clearly different and identifies W306 as the oxidized species. These findings set an upper limit of 10 ns for electron transfer from W306 to $W359^{\bullet+}$ in wildtype DNA photolyase, consistent with previous, more indirect evidence [Aubert, C.; Vos, M. H.; Mathis, P.; Eker, A. P. M.; Brettel, K. *Nature* **2000**, *405*, 586−590].

Introduction

DNA photolyase (see refs 1–3 for recent reviews) is a flavoprotein that repairs major UV-induced lesions in DNA, the cyclobutane−pyrimidine dimers (CPD). The repair reaction is triggered by blue or near-UV light and involves electron transfer to the CPD from the photoexcited flavin adenine dinucleotide (FAD) cofactor in its fully reduced form ($FADH^{-}$). A distinct photoreaction, known as photoactivation, restores the fully reduced form of the flavin cofactor from its semireduced form, the neutral radical $FADH^{\bullet}$. The latter state is rather stable in photolyase (in contrast to flavins in solution), and purified photolyases typically contain the flavin cofactor in this form, presumably because of oxidation of $FADH^{-}$ during the isolation procedure. Although the physiological role of photoactivation is not established,[4] its reaction mechanism is of considerable interest because it involves long-range electron transfer to the excited flavin radical along a chain of three tryptophan residues, FAD−W382−W359−W306 (for *E. coli* photolyase). Long-range electron transfer involving intrinsic amino acids is crucial for other enzymes, notably ribonucleotide reductase;[5] compared to the latter, photolyase offers the advantage that the reactions can be readily studied with high time resolution because they are intrinsically light-induced and can be triggered by a laser pulse.

Thus, the current knowledge on photoactivation is largely based on transient absorption studies combined with site-directed mutagenesis of tryptophan residues.[6–10] According to these studies, photoactivation of *E. coli* photolyase proceeds as follows: upon absorption of a photon, the excited state of $FADH^{\bullet}$ abstracts an electron from W382 (also denoted $_{382}$TrpH, where H denotes the N1 proton) in ∼30 ps (a biphasic description of transient absorption data with time constants of 11 and 42 ps led Wang and co-workers[11] to suggest that a phenylalanine (F366) might be oxidized in addition to W382; see ref 9 for a critical discussion). The cation radical $_{382}TrpH^{\bullet+}$ is then reduced by $_{359}$TrpH, and $_{359}TrpH^{\bullet+}$ is subsequently reduced by the solvent-exposed residue $_{306}$TrpH in presumably less than 10 ns. $_{306}TrpH^{\bullet+}$ releases a proton into the aqueous phase in ∼200 ns. The remaining neutral radical $_{306}Trp^{\bullet}$ can be re-reduced by extrinsic electron donors, thus stabilizing the fully reduced $FADH^{-}$. Although the tryptophan cation radical has a pronounced absorption band centered at ∼570 nm, the electron transfer between the tryptophan residues could not be monitored directly so far (the upper limit of 10 ns was deduced from the lack of a lag phase of $_{306}TrpH^{\bullet+}$ deprotonation). This is because the absorption changes due to the reduction of $_{382}TrpH^{\bullet+}$ are compensated by those due to the concomitant oxidation of

* Corresponding author. Phone: (33) 1 69 08 90 14. Fax: (33) 1 69 08 87 17. E-mail: Martin.Byrdin@cea.fr.
† CEA.
‡ CNRS.
§ Permanent address: Centre de Biophysique Moléculaire, CNRS UPR 4301, conventionnée avec l'Université d'Orléans, Rue C. Sadron, 45071 Orleans Cedex 2, France.
∥ Permanent address: Laboratoire de Chimie Physique, CNRS UMR 8000, Universite Paris XI, Bat 349, 91405 Orsay Cedex, France.
⊥ Erasmus University Medical Centre.

10.1021/jp711435y CCC: $40.75
Published on Web 05/10/2008

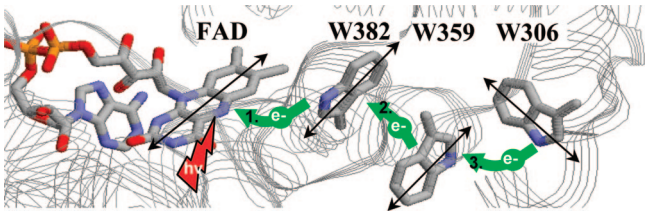

Figure 1. Extract from the crystal structure of *E.coli* photolyase[12] showing the members of the photoactivation electron-transfer chain FAD−W382−W359−W306. The numbers in the arrows indicate the temporal order of the electron-transfer steps. Note that the long axes of W382 and W359 are rather parallel to each other whereas that of W306 is almost perpendicular to both of them.

$_{359}$TrpH and, correspondingly, for the reduction of $_{359}$TrpH$^{\bullet+}$ and the oxidation of $_{306}$TrpH.

To overcome this difficulty, it is interesting to exploit the fact that, according to the crystal structure,[12] the tryptophans in question are differently oriented within the protein (see Figure 1). By using a linearly polarized laser flash, we preferentially excited photolyases oriented with their FADH$^{\bullet}$ transition dipole moment parallel to the laser-flash polarization direction (photoselection). Monitoring the flash-induced absorption changes with polarized light should then allow us to distinguish between tryptophan radicals that differ in the orientation of their transition dipoles relative to the FADH$^{\bullet}$ transition dipole. Both for the neutral flavinyl radical and for the tryptophanyl radical (in either protonated or unprotonated form), the red-most transition dipole is nearly parallel to the long molecular axis.[13,14] Hence, the radical of W306 (long axis at ∼75° to the long axis of the flavin) should be well distinguishable from the radicals of W359 (∼30°) and W382 (∼45°).

Because we could not resolve the electron transfer from $_{306}$TrpH to $_{359}$TrpH$^{\bullet+}$ at the current time resolution of our polarized transient absorption setup (10 ns), we mutated W306 to redox-inert phenylalanine, thus pruning the electron-transfer chain behind W359. We show that the anisotropy spectrum of the initial absorption changes is in line with W359 being oxidized. The corresponding spectrum in wildtype photolyase is clearly different and identifies W306 as the oxidized species. This difference should allow us to resolve the kinetics of electron transfer from $_{306}$TrpH to $_{359}$TrpH$^{\bullet+}$ in future polarized transient absorption experiments with improved time resolution.

Materials and Methods

Anisotropy. There exist several concepts to describe the degree of optical polarization of a system (for review, see, e.g., ref 15). The one we adopt here to describe polarization effects in flash absorption spectrocopy is that of (polarizational) anisotropy r. In analogy to polarized fluorescence spectroscopy, anisotropy r is defined here as the difference between absorption changes measured with light polarized parallel ($\Delta A_{||}$) and perpendicular ($\Delta A_{\perp}$) to the excitation polarization direction, normalized to the sum of one parallel and two perpendicular contributions.[16]

$$r = \frac{\Delta A_{||} - \Delta A_{\perp}}{\Delta A_{||} + 2\Delta A_{\perp}} \tag{1}$$

The denominator represents three times the isotropic signal ΔA_{iso}, that is, the signal that would be observed after complete rotational randomization (depolarization) of the sample. The signal measured at the magic angle (54.7°) to the excitation polarization is identical to the isotropic signal.

$$\Delta A_{m.a.} = \Delta A_{iso} = \frac{\Delta A_{||} + 2\Delta A_{\perp}}{3} \tag{2}$$

For systems composed of several absorbing species i, the total anisotropy r_{tot} is related to the anisotropies r_i of each species by the simple rule

$$r_{tot} = \frac{\sum r_i \Delta A_{i,iso}}{\Delta A_{tot,iso}} \tag{3}$$

The anisotropy loss due to Brownian rotational diffusion is described by a (multi)exponential decay, the number of exponential components depending on the symmetry of the system. For a sphere, the anisotropy decay is described by a single exponential

$$r(t) = r_0 \exp(-t/\tau) \tag{4}$$

where r_0 is the anisotropy at $t = 0$. In practice, the deviations of globular proteins from the spherical form are often not big enough to resolve additional components with separate lifetimes. The lifetime of rotational diffusion τ is determined by the temperature T and the viscosity η of the solvent, as well as the radius R of the (idealized) sphere representing the solute (k is Boltzmann's constant).

$$\tau = \frac{4\pi R^3 \eta}{3kT} \tag{5}$$

A rough estimate, assuming a spherical photolyase of molecular mass 54 kDa and a mass density of 1 g/cm^3, would yield a τ value of about 30 ns (at room temperature in water). Hence, polarization effects should be detectable with the 10 ns time-resolution transient absorption setup described below.

For conditions under which a single transition is excited and (another) single transition is detected, the observed anisotropy r depends on the angle β between the two transitions' dipoles:

$$r = \frac{3\cos^2\beta - 1}{5} \tag{6}$$

For parallel transitions ($\beta = 0$), r is maximal ($r = 0.4$, corresponding to $\Delta A_{||}/\Delta A_{\perp} = 3$), and for perpendicular transitions ($\beta = 90°$), r is minimal ($r = -0.2$, corresponding to $\Delta A_{||}/\Delta A_{\perp} = 0.5$), passing zero at $\beta = 54.7°$ ($\Delta A_{||} = \Delta A_{\perp}$). If more than one transition is detected (as is in general the case for electron-transfer processes, where both donor and acceptor can give rise to absorbance changes), compensations between the different contributions to $\Delta A_{tot,iso}$ can lead to a small denominator in eq 3 and hence to anisotropy values outside the range $-0.2 \le r_{tot} \le 0.4$. For photolyase, we therefore expect anisotropy fingerprints in the spectral region between 500 and 600 nm, where the absorption increase due to the formation of the tryptophanyl radical can compensate a large part of the absorption decrease due to the reduction of FADH$^{\bullet}$.

Time-Resolved Polarized Absorption Spectroscopy. Polarized transient absorption data in the wavelength region from 420 to 660 nm were recorded with a time resolution of 10 ns on the setup described recently[10] by using vertically polarized excitation and setting the detection light polarizer alternatingly to vertical (for $\Delta A_{||}$) and horizontal (for $\Delta A_{\perp}$) orientations. At each detection wavelength, typically, 32 absorption transients were averaged for each polarizer setting. Excitation pulses of 5 ns fwhm and 30 mJ/cm^2 at 640 nm were provided by a Nd:YAG pumped optical parametrical oscillator (Brillant B/Rainbow, Quantel, France).

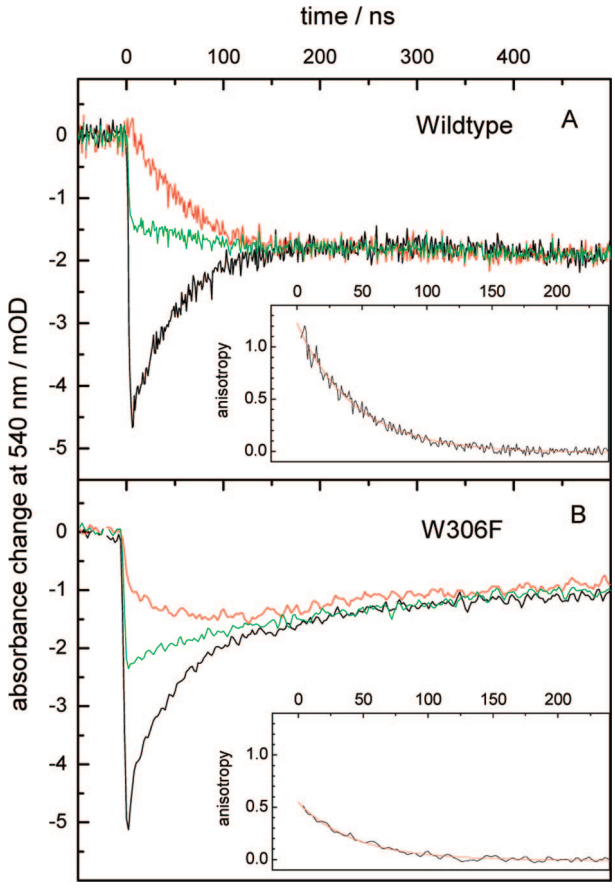

Figure 2. Time traces of absorbance changes in wildtype (A) and W306F mutant (B) photolyase samples after a vertically polarized laser flash at 640 nm. Detection was at 540 nm with polarizer set vertical ($\Delta A_{\parallel}$, black), at magic angle ($\Delta A_{m.a.}$, green) and horizontal ($\Delta A_{\perp}$, red). The inset shows anisotropy decay kinetics as calculated according to eq 1 (black) and fitted according to eq 4 (red).

In order to obtain anisotropy values (as defined in eq 1) from the measured absorption transients, we first considered two straightforward approaches: (a) fitting each transient by a multiexponential decay and then calculating anisotropies from the best fit curves or (b) inversely, first constructing anisotropy decays from the raw data and then obtaining best values for the anisotropy from fits to these meta-data. For data with superior signal-to-noise ratio, both approaches should yield equivalent results. In practice, approach b turned out to have the drawback that the division of noisy raw data by other noisy raw data often strongly degraded the signal-to-noise ratio. In approach a, direct fitting of the raw data was often not very reliable because it required at least two not-well-separated exponential components (one for the anisotropy decay and one for the chemical reaction) and a constant (for long-lived reaction products). In contrast, the anisotropy decay to be fitted in approach b should be monoexponential (eq 4) and hence more easy to fit. The best way to profit from this advantage without suffering from the accompanying drawback turned out to be the following: isotropic kinetic data were constructed from raw data according to eq 2 and fitted by one exponential and a constant. These noise-free fitted curves were used in the denominator of eq 1 to construct pure anisotropy decays (see insets in Figure 2) without degrading the signal-to-noise ratio of the raw data. Because of small fluctuations in the excitation flash energy, the measured $\Delta A_{\parallel}$ and $\Delta A_{\perp}$ traces did not always reach exactly the same level after decay of the polarization (see, e.g., Figure 2B). To ensure a decay of the anisotropy to zero, these slight differences were corrected for by normalization of the corresponding data sets at times >400 ns.

Monoexponential fits to the thus obtained anisotropy kinetics yielded robust amplitude values. Fitting was started 15 ns after time zero (defined as the peak position of the response of our detection system to the excitation pulse). Initial anisotropy values were obtained by extrapolating the fit curves back to time zero.

In a separate series of experiments aimed at determining the angle between the red-most and the other visible transition dipoles of $FADH^{\bullet}$ in wildtype photolyase, the excitation wavelength was varied in 10 nm steps between 480 and 630 nm, and flavin-only flash-induced polarized absorbance changes were recorded at 650 nm, where the flavin radical $FADH^{\bullet}$ is expected to be the only absorbing species.

Sample Preparation. Wildtype and W306F mutant photolyase were prepared as described previously.[10] For measurements, samples containing typically 40 μM protein and no reductant in standard measuring buffer (20 mM Tris·HCl (pH 7.4) and 0.2 M NaCl) were placed in a 4 mm (exciting light path) × 10 mm (detection light path) cuvette held at 12 °C.

Results and Discussion

Figure 2 compares absorbance-change kinetics at 540 nm of wildtype (A) and W306F mutant (B) photolyase after excitation by laser flashes at 640 nm at different polarizations of the detecting light. The isotropic kinetics (measured at magic angle, green traces) have been studied previously[7,10] and can be understood as follows: in wildtype photolyase, electron transfer to excited $FADH^{\bullet}$ along the chain W382−W359−W306 (see Figure 1) leads to the formation of $FADH^{-}$ and $_{306}TrpH^{\bullet+}$ in presumably less than 10 ns. These reactions give rise to the instrument-limited initial absorbance decrease at 540 nm seen in Figure 2A. The absorbance decrease results from bleaching of $FADH^{\bullet}$ that is partly compensated by the absorption of $_{306}TrpH^{\bullet+}$ (see also Figure 4). $_{306}TrpH^{\bullet+}$ subsequently deprotonates with a time constant of ∼200 ns, forming the neutral radical $_{306}Trp^{\bullet}$. This reaction is accompanied by a further absorbance decrease at 540 nm, as Trp° absorbs less at this wavelength than $TrpH^{\bullet+}$. The state ($FADH^{-}$ $_{306}Trp^{\bullet}$) is much longer-lived than the present time scale and finally decays by charge recombination in ∼10 ms under our experimental conditions. In the W306F mutant photolyase sample, the terminal tryptophan W306 has been replaced by an isosteric phenylalanine that is much harder to oxidize, thus leaving the electron-transfer chain cut off after the second tryptophan W359. We have shown[10] that the W359 radical formed in the W306F mutant photolyase is in its neutral form ($_{359}Trp^{\bullet}$) already at 10 ns after excitation, the earliest time accessible at our present time resolution. The state ($FADH^{-}$ $_{359}Trp^{\bullet}$) recombines in ∼1 μs (see Figure 2 of ref 10 for a more complete presentation of the isotropic signal recovery).

The kinetics measured with parallel (black) and perpendicular (red) polarization deviate strongly from the isotropic kinetics during the first ∼100 ns and then join the isotropic traces. The relative deviations are more pronounced for wildtype than for W306F mutant photolyase, but even for the latter, the $\Delta A_{\parallel}/\Delta A_{\perp}$ ratio at early times clearly exceeds the value of 3 (corresponding to an anisotropy value $r = 0.4$), the upper limit when a single transition is detected. This is not unexpected because two species ($FADH^{\bullet}$ and a tryptophanyl radical) contribute with opposite signs to the absorbance changes at 540 nm.

For quantitative analysis, we combined the $\Delta A_{\parallel}$ and $\Delta A_{\perp}$ traces according to eq 1 to obtain pure anisotropy decay curves (insets in Figure 2). These curves are well described by

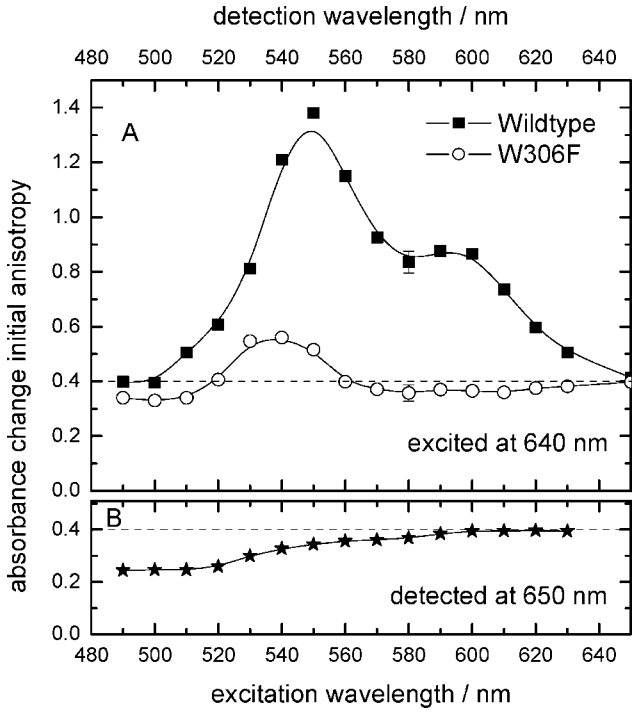

Figure 3. (A) Spectra of initial anisotropies of wildtype and W306F mutant photolyase upon excitation at 640 nm. The data points were obtained from the analysis (see Materials and Methods) of kinetic traces as those shown in Figure 2, measured at various detection wavelengths. (B) Flavin-only initial-anisotropy spectrum of wildtype photolyase obtained from an excitation scan with detection at 650 nm. The error bars (shown at 580 nm) present typical errors estimated from the rms noise of kinetic traces as those shown in the insets of Figure 2. For the data in panel B, the error (±0.006) is smaller than the symbol size.

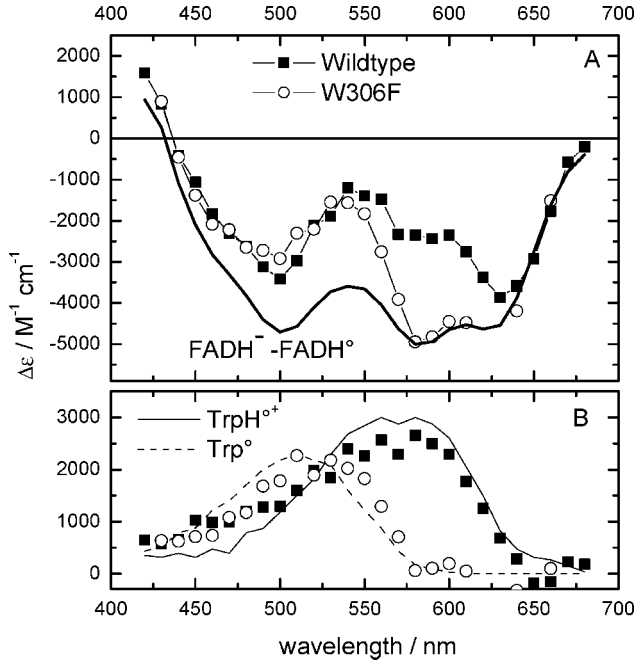

Figure 4. Additional spectra used in the evaluation of eq 7. (A) Symbols connected by thin lines: isotropic initial (extrapolated to time zero) absorbance changes in wildtype and W306F mutant photolyase, detected at magic angle (54.7°) with respect to the vertically polarized 640 nm excitation flash. Thick line: steady-state absorption changes upon photoreduction[10] of $FADH^{\bullet}$ to $FADH^{-}$ in wildtype photolyase, scaled to $\Delta\epsilon = -5000\ M^{-1}\cdot cm^{-1}$ at 580 nm. The three spectra were normalized at 650 nm. (B) Symbols: difference between the corresponding symbols and the solid line in panel A. Lines: literature[17] spectra of protonated (solid) and deprotonated (dashed) tryptophanyl radicals in aqueous phase. Typical amplitude errors, as estimated from the rms noise of magic-angle kinetic traces as those shown in Figure 2, are in the order of $\pm 100\ M^{-1}\cdot cm^{-1}$, i.e., comparable to the symbol size.

monoexponential decays. This allows us to extract reliable values for the initial absorbance-change anisotropy. The fits yielded values r_0 of 1.2 and 0.55 and decay time constants τ of 47 and 48 ns for wildtype and W306F mutant photolyase, respectively. According to eq 5, an anisotropy decay with $\tau =$ 48 ns in aqueous solution at 12 °C corresponds to a dynamic radius of 3.3 nm for a spherical protein. This has to be compared to the ca. 3 × 4 × 8 nm dimensions of monomeric photolyase as derived from the crystal structure.[12] The fact that the anisotropy decay could be well fitted by a single exponential and yielded a reasonable protein size indicates that the spherical shape approximation is adequate, even for a prolate protein like photolyase.

Dedicated treatments (as described in Materials and Methods) of the kinetic traces measured at wavelengths between 650 and 490 nm (lower wavelengths were excluded because of complications due to the absorption of $FADH^{-}$) resulted in initial anisotropy spectra as shown in Figure 3A. As expected, both wildtype and W306F mutant photolyase samples show initial anisotropies close to 0.4 in the spectral regions where absorption of the tryptophanyl radicals is negligible (above 570 nm for $_{359}Trp^{\bullet}$ in W306F mutant photolyase and at 650 nm for $_{306}TrpH^{\bullet+}$ in wildtype photolyase), so that the only contribution to the flash-induced absorbance change is due to depletion of the $FADH^{\bullet}$ ground-state absorption, that is, the same transition that has been excited. Hence, $\beta = 0$ and $r = 0.4$ according to eq 6. The strong deviations from $r = 0.4$ at lower wavelengths are expected to be mainly due to contributions from the tryptophanyl radicals. In addition, one has to take into account that the short-wavelength transition dipoles of $FADH^{\bullet}$ may not be perfectly parallel to the excited red-most transition. Eaton et al.[14] reported an angle of 20° between the long-wavelength alpha band and the short-wavelength beta band of a flavinyl radical in flavodoxin (containing the flavin mononucleotide radical $FMNH^{\bullet}$ instead of $FADH^{\bullet}$ in photolyase).

In order to be able to account for a wavelength-dependent flavin anisotropy, we detected flavin-only flash-induced polarized absorbance changes at 650 nm in wildtype photolyase as a function of the excitation wavelength. The resulting initial anisotropy (Figure 3B) decreases from 0.4 above 600 nm to 0.25 around 500 nm, which corresponds, according to eq 6, to an angle of 30° between the red-most and the 500 nm band, in reasonable agreement with the flavodoxin data.[14]

Thus, knowing the contribution of the flavinyl radical to our measured anisotropy spectra, we can extract information on the tryptophanyl radicals. The basis for this treatment is given by eq 3, stating how the total anisotropy is related to the anisotropies of the components, and eq 6, relating the anisotropy of a single detected transition to the angle β between the excited and the detected transition dipoles.

Applying eq 3 to our case, we obtain a relation containing six different spectra:

$$r_{tot}(\lambda) = \frac{r_{flavin}(\lambda)\Delta A_{flavin,iso}(\lambda) + r_{trp}(\lambda)\Delta A_{trp,iso}(\lambda)}{\Delta A_{tot,iso}(\lambda)} \quad (7)$$

For each of the two samples studied, four of the six spectra in eq 7 have been measured directly: $r_{tot}(\lambda)$ (Figure 3A), $\Delta A_{tot,iso}(\lambda)$ (Figure 4A), $r_{flavin}(\lambda)$ (Figure 3B), and $\Delta A_{flavin,iso}(\lambda)$ (Figure 4A, thick line). The isotropic tryptophan contributions

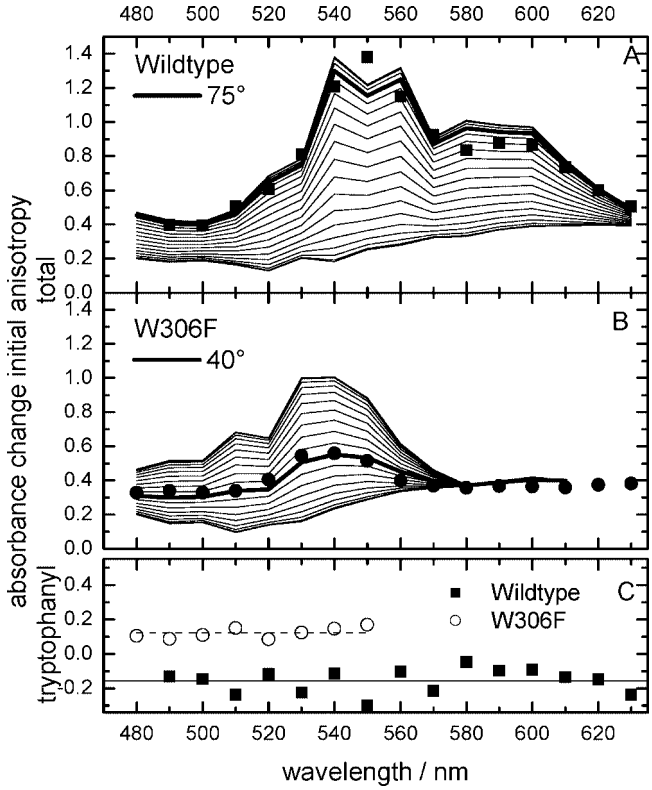

Figure 5. Extraction of the angles between excited and detected transition dipole moments. (A) and (B) Lines: absorption-change anisotropies r_{tot} simulated according to eq 7 for different angles β (from 0 (bottom) to 90° (top) in 5° intervals) between the red-most FADH$^{\bullet}$ transition dipole and the visible tryptophanyl transition dipoles of $_{306}$TrpH$^{\bullet+}$ (A) and $_{359}$Trp$^{\bullet}$ (B). Symbols: initial anisotropies measured in wildtype (A) and W306F mutant (B) photolyase, reproduced from Figure 3A. (C) Tryptophanyl absorption-change anisotropies r_{trp} calculated from experimental data (according to eq 7) for wildtype (squares) and W306F mutant (circles) photolyase. Average values are indicated by horizontal lines.

$\Delta A_{trp,iso}(\lambda)$ (Figure 4B, symbols) were obtained as the differences between the total isotropic spectra, $\Delta A_{tot,iso}(\lambda)$, and the isotropic spectrum for FADH$^{\bullet}$ reduction, $\Delta A_{flavin,iso}(\lambda)$; they agree reasonably well with solution spectra of TrpH$^{\bullet+}$ and Trp$^{\bullet}$ (lines) found in the literature.[17] Thus, the only unknown spectra are the anisotropy spectra $r_{trp}(\lambda)$ of the tryptophanyl radicals ($_{306}$TrpH$^{\bullet+}$ in wildtype and $_{359}$Trp$^{\bullet}$ in W306F mutant photolyase). According to eq 6, they are directly related to the angles β between the detected optical transitions of these tryptophanyl radicals and the excited FADH$^{\bullet}$ transition. In the following, we develop two different approaches to extract these angles from our experimental data (extrapolated to $t = 0$).

In approach a, we simulate total anisotropy spectra $r_{tot}(\lambda)$ according to eq 7 for both wildtype and W306F mutant photolyase assuming different angles β (from 0 to 90° in steps of 5°) between the detected tryptophanyl radical transition and the excited flavin transition and compare them with the experimental total anisotropy spectra in order to determine the best values of β (Figure 5A,B). The simulations used the isotropic tryptophan contributions $\Delta A_{trp,iso}(\lambda)$ from Figure 4B (symbols) and all directly measured spectra listed above except $r_{tot}(\lambda)$. It was assumed that the transition dipole orientations are independent of the wavelength within the main visible absorption bands of the tryptophanyl radicals in the 480−630 nm range considered here. For both samples, the simulated anisotropy spectra (lines in Figure 5A,B) depend strongly on the assumed orientation of the tryptophanyl transitions in the region where the respective tryptophanyl radicals absorb. This is because of the strong variation of r_{trp} as a function of β (eq 6). The effect is the strongest in the regions were $\Delta A_{tot,iso}(\lambda)$ is small because of compensation between negative and positive absorbance changes due to flash-induced FADH$^{\bullet}$ ground-state depletion and tryptophanyl radical formation (around 550 nm for wildtype and around 530 nm for W306F mutant photolyase; see Figure 4). Among the simulated anisotropy spectra, those for $\beta = 75°$ for wildtype and $\beta = 40°$ for W306F mutant photolyase (highlighted by thicker lines in Figures 5A,B) agree best with the experimental spectra (symbols). Taking into account the uncertainties for both measured and calculated anisotropies, we estimate $60° < \beta < 90°$ for wildtype photolyase and $35° < \beta < 50°$ for W306F mutant photolyase.

A substantial difference between the orientations of the tryptophanyl radical transition dipoles of the two samples was expected because of the different orientations of W359 and W306 known from the crystal structure (see Figure 1). The fact that, for each sample, the experimental data do largely lie close to a single simulated spectrum confirms the validity of our approach.

In approach b, we calculated $r_{trp}(\lambda)$ directly from eq 7 by using all of the five other spectra determined as described above. The wavelengths where the absorption of the respective tryptophanyl radicals is small compared to that of FADH$^{\bullet}$ (>630 nm for $_{306}$TrpH$^{\bullet+}$ in wildtype and >560 nm for $_{359}$Trp$^{\bullet}$ in W306F mutant photolyase) were omitted, because the calculation of $r_{trp}(\lambda)$ involves a division by $\Delta A_{trp,iso}(\lambda)$. The thus calculated anisotropy spectra of the two tryptophanyl radicals (Figure 5C) are flat within the scattering of the data, justifying a posteriori the assumption of wavelength-independent orientations of the tryptophanyl radical transitions in approach a. The averaged tryptophanyl anisotropies of -0.156 ± 0.07 and 0.123 ± 0.03 correspond (eq 6) to angles β of 74° (+16°, −9°) and 43°

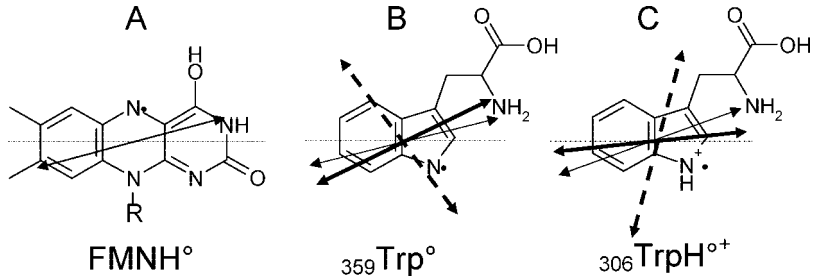

Figure 6. Orientation of transition dipole moments within the molecular frame of species relevant to this work. (A) Red-most transition of FMNH$^{\bullet}$ in a flavodoxin (from ref 14). (B) and (C) Visible transition of tryptophanyl radicals. Thick arrows: the two possible in-plane orientations in $_{359}$Trp$^{\bullet}$ (B) and $_{306}$TrpH$^{\bullet+}$ (C) derived in the present work. Thin arrow: predictions from time-dependent density functional theory (DFT) calculations[13] for Trp$^{\bullet}$ (B) and TrpH$^{\bullet+}$(C) in gas phase. The long molecular axes of all species were aligned horizontally (dash-dotted).

(± 3°) between the excited flavin transition and the detected transition of $_{306}TrpH^{\bullet+}$ in wildtype and $_{359}Trp^{\bullet}$ in W306F mutant photolyase, respectively.

These angles can be related to structural data from X-ray crystallography.[12] This requires knowledge of the transition dipole orientations within the molecular frame of the species involved (Figure 6).

On the basis of the measurement of flavodoxin crystals containing FMN in neutral radical form ($FMNH^{\bullet}$), Eaton et al.[14] concluded that the red-most transition dipole moment in the neutral flavinyl radical lies in the plane of the molecule and forms an angle of 15° with its long axis (Figure 6A). For the tryptophanyl radical, time-dependent DFT calculations[13] on both the protonated and deprotonated forms in gas phase suggest an in-plane orientation of the visible transition at an angle of 14° with the long molecule axis for the deprotonated and of 20° for the protonated tryptophanyl radical (thin arrows in Figure 6B,C). Using these values and the coordinates from the 1dnp.pdb structure file gives angles of 79 and 35° between the involved transitions of the tryptophanyl and flavinyl radicals for wildtype and W306F mutant photolyase, respectively. These angles are in reasonable agreement with the angles deduced from our measurements (74 and 43°). Inversely, on the basis of the orientation of the flavinyl transition dipole determined in ref 14, our measurements can be used to deduce the orientation of the transition dipole moments within the tryptophan molecular planes. Because of the geometry of the system, there are two possible orientations fulfilling the condition imposed by our results (thick arrows in Figure 6B,C). For both $_{359}Trp^{\bullet}$ and $_{306}TrpH^{\bullet+}$, one of these two orientations (solid thick arrows) is closer to the in silico result[13] (thin arrows) and closer to the long molecular axis (26 and 6° for $_{359}Trp^{\bullet}$ and $_{306}TrpH^{\bullet+}$, respectively) than the alternative orientations (dashed arrows; 127 and 75°, respectively).

Conclusion

The ultimate aim of this study was to open a way for determining the rates of electron transfer between the tryptophan residues in wildtype photolyase. From the present results, we anticipate that electron transfer from $_{306}TrpH$ to $_{359}TrpH^{\bullet+}$ is related to a change of the orientation of the tryptophanyl radical transition from ~43 ($_{359}TrpH^{\bullet+}$) to ~74° ($_{306}TrpH^{\bullet+}$) with respect to the red-most transition dipole of $FADH^{\bullet}$. This transfer should hence be accompanied by a pronounced increase of absorbance-change anisotropy around 550 nm, going from $r \approx 0.8$ (45° spectrum for a protonated tryptophanyl in Figure 5A) to $r \approx 1.2$ (symbols in Figure 5A). At the present time-resolution of 10 ns, no such increase in anisotropy could be resolved (see Figure 2A, inset), in line with a previous conclusion that $_{306}TrpH$ is oxidized in less than 10 ns.[7] A new setup with an improved time resolution is under construction in our laboratory, aiming at the detection of this crucial electron-transfer step by time-resolved polarized absorption spectroscopy.

Acknowledgment. This work was supported by Agence Nationale de la Recherche grant no. ANR-05-BLAN-0304-01 and The Netherlands Organization for Scientific Research (NWO-CW 700.51.304). We thank Dr M. Modesti for valuable help in preparing the mutant photolyase gene, Drs. A. Yasui and K. Yamamoto for providing us with the pKE plasmid and *E. coli* KY29 strain, respectively, and Dr. J. H. J. Hoeijmakers for his continuous interest in this project.

Abbreviations

CPD, cyclobutane pyrimidine dimer;
$FADH^{\bullet}$, singly reduced neutral radical state of FAD;
$FADH^{-}$, doubly reduced state of FAD;
TrpH, neutral Tryptophan, where H denotes the N1 proton;
$TrpH^{\bullet+}$, Tryptophan cation radical state ($TrpH - e^{-}$);
$Trp^{\bullet}$, Tryptophan neutral radical state ($TrpH\ {}^{-}e^{-} - H^{+}$);
DFT, density functional theory.

References and Notes

(1) Sancar, A. *Chem. Rev.* **2003**, *103*, 2203.
(2) Weber, S. *Biochim. Biophys. Acta* **2005**, *1707*, 1.
(3) Byrdin, M.; Sartor, V.; Eker, A. P. M.; Vos, M. H.; Aubert, C.; Brettel, K.; Mathis, P. *Biochim. Biophys. Acta* **2004**, *1655*, 64.
(4) Kavakli, I. H.; Sancar, A. *Biochemistry* **2004**, *43*, 15103.
(5) Reece, S. Y.; Hodgkiss, J. M.; Stubbe, J.; Nocera, D. G. *Philos. Trans. R. Soc., Ser. B* **2006**, *361*, 1351.
(6) Li, Y. F.; Heelis, P. F.; Sancar, A. *Biochemistry* **1991**, *30*, 6322.
(7) Aubert, C.; Vos, M. H.; Mathis, P.; Eker, A. P. M.; Brettel, K. *Nature* **2000**, *405*, 586.
(8) Byrdin, M.; Eker, A. P. M.; Vos, M. H.; Brettel, K. *Proc. Natl. Acad. Sci. U.S.A.* **2003**, *100*, 8676.
(9) Lukacs, A.; Eker, A. P. M.; Byrdin, M.; Villette, S.; Pan, J.; Brettel, K.; Vos, M. H. *J. Phys. Chem. B* **2006**, *110*, 15654.
(10) Byrdin, M.; Villette, S.; Eker, A. P. M.; Brettel, K. *Biochemistry* **2007**, *46*, 10072.
(11) Wang, H.; Saxena, C.; Quan, D.; Sancar, A.; Zhong, D. *J. Phys. Chem. B* **2005**, *109*, 1329.
(12) Park, H. W.; Kim, S. T.; Sancar, A.; Deisenhofer, J. *Science* **1995**, *268*, 1866.
(13) Crespo, A.; Turjanski, A. G.; Estrin, D. A. Chem. Phys. Lett. 2002, *365*, 15 and D. Estrin, personal communication.
(14) Eaton, W. A.; Hofrichter, J.; Makinen, M. W.; Andersen, R. D.; Ludwig, M. L. *Biochemistry* **1975**, *14*, 2146.
(15) Kawski, A. *Crit. Rev. Anal. Chem.* **1993**, *23*, 459.
(16) Causgrove, T. P.; Yang, S. M.; Struve, W. S. *J. Phys. Chem.* **1988**, *92*, 6121.
(17) Solar, S.; Getoff, N.; Surdhar, P. S.; Armstrong, D. A.; Singh, A. *J. Phys.Chem.* **1991**, *95*, 3639.

JP711435Y